Journal of Magnetics 16(4), 427-430 (2011) http://dx.doi.org/10.4283/JMAG.2011.16.4.427

Characteristics of Barkhausen Noise Properties and Hysteresis Loop on Tensile Stressed Rolled Steels

Hiroaki Kikuchi*, Katsuyuki Ara, Yasuhiro Kamada, and Satoru Kobayashi

Faculty of Engineering, Iwate University, Morioka 020-8551, Japan

(Received 9 August 2011, Received in final form 24 September 2011, Accepted 4 October 2011)

The rolled steels for welded structure applied tensile stress have been examined by means of magnetic Barkhausen noise (MBN) method and of a physical parameter obtained from a hysteresis loop. The behaviors of MBN parameters and coercive force with tensile stress were discussed in relation to microstructure changes. There is no change in MBN parameters and coercive force below yield strength. The coercive force rises rapidly with tensile stress above yield strength. On the other hand, the rms voltage and the peak in averaged rms voltage take a maximum around yield strength and then decreases. The magnetomotive force at peak in the averaged rms voltage shows a minimum around yield strength. These phenomena are attributed to the combined effects of cell texture and dislocation density. In addition, the behaviors of MBN parameters around yield strength may be reflected by the localized changes in strain field due to the formation of dislocation tangles.

Keywords : barkhausen noise, coercive force, tensile stress, dislocation, microstructure

1. Introduction

Since magnetic properties such as magnetic Barkhausen noise (MBN) and parameters obtained from hysteresis loop are sensitive to microstructures of ferromagnetic materials [1], they have been used as tools for characterization and nondestructive evaluation of ferromagnetic materials. The MBN is a phenomenon that occurs when magnetic domain walls are unpinned from obstructions such as grain boundaries, dislocations and inclusions in a ferromagnetic material, which is the reason why MBN is very sensitive to microstructure changes of ferromagnetic materials. There are many investigations of MBN signal changes under various conditions like fatigue [2], irradiation [3], residual stress [4], creep [5] and so on and it has been proved to be sensitive to grain size [6], composition [7], hardness [8], etc.

When magnetic methods are applied for the monitoring of degradation in constructed structures, mechanical properties of the steels should be evaluated. Therefore, the behaviors of those magnetic parameters should be clarified when mechanical properties change. In order to change mechanical properties of steels, tensile test is often used. Thus, in this work, plates made of rolled steels for welded structure were prepared and were deformed using tensile test. Then, magnetic measurements (MBN and hysteresis loop) were analyzed to understand behaviors of MBN parameters and of coercive force depending on the tensile stresses and microstructure changes taking place during test.

*Corresponding author: Tel: +81-19-621-6890
Fax: +81-19-621-6890, e-mail: hkiku@iwate-u.ac.jp

2. Experimental Procedure

The rolled steel samples for welded structure, SM490A, were used in this study. The chemical composition of the steel is listed in Table 1. Fig. 1 shows the dimensional details of tensile test specimens. Those specimens were elastically and plastically deformed with the tensile stresses of 299, 457 and 518 MPa. The yield strength of SM490A steel is 450 MPa and the tensile strength of that is 580 MPa [9]. After released tensile stresses, MBN parameters and hysteresis loop characteristics were measured.

Tensile test specimens were magnetized parallel to the direction applied tensile stresses using a single-yoke

Table 1. Chemical composition of SM490A steel (wt.%).

C	Si	Mn	P	S	Fe
0.18	0.04	1.19	0.013	0.005	bal.

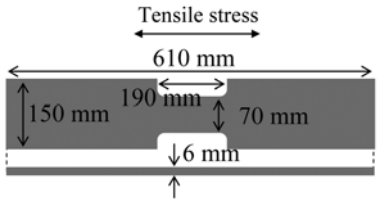

Fig. 1. Dimension of plate (unit: mm).

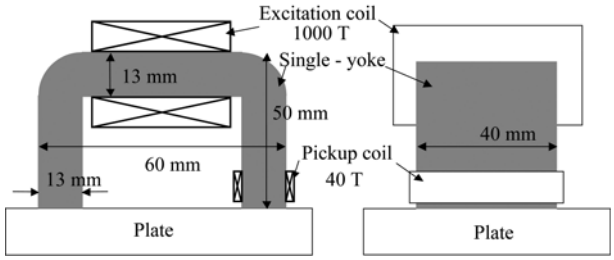

Fig. 2. Schematic view and dimension of single-yoke probe.

probe. The single-yoke probe was composed of a U-type Fe-Si yoke, a magnetizing coil and a pickup coil as shown in Fig. 2. The dimension of the yoke probe is also shown in Fig. 2. The number of the magnetizing coil is 1000 turns and that of the pickup coil 40 turns. The original MBN signals were detected by an air-core coil with 737 turns and 80 mm^2, attached on the surface of plates. The measurement system for MBN and hysteresis loop is illustrated in Fig. 3. A triangular wave current of 1 Hz is used to magnetize plates for MBN measurement and 0.05 Hz for hysteresis loops. The original MBN signals induced at air-core coil were amplified (60 dB), band pass filtered (100-200 kHz), and finally sampled with sampling rate of 100 kHz. On the other hand, induced voltage at pickup coil on the single-yoke was amplified (20 dB), low pass filtered (cut-off frequency is 50 Hz), and finally sampled with sampling rate of 100 Hz.

Here, magnetomotive force, NI, is used to evaluate MBN and hysteresis loop, where I is a magnetizing current and N the number of magnetizing coil, because the magnetic field intensity in the plates has distribution and it is difficult to measure the field intensity precisely.

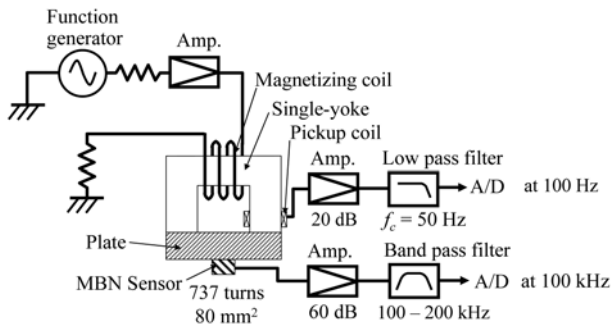

Fig. 3. MBN and hysteresis loop measurement setup.

The induced voltage at the pickup coil is proportional to the change of magnetic flux concentrated in the magnetic circuit. The magnetic flux, Φ, was calculated by integration of induced voltage at the pickup coil. Since it is difficult to decide equivalent cross sectional area of the plates, we use the magnetic flux Φ for the evaluation of hysteresis loop. As a result, a hysteresis loop (Φ–I loop) was obtained.

A MBN parameter dependency on tensile stresses was studied in terms of rms voltage. The rms voltage, RMS_{MBN}, is defined as the root mean value of the voltage signal to be described by the following equation.

$$RMS_{MBN} = \sqrt{\frac{1}{T}\int_0^T V_{MBN}^2 dt} \quad (1)$$

where V_{MBN} is original MBN signal and T is a half period of magnetizing cycle.

3. Experimental Results

Fig. 4 shows the hysteresis loops obtained from SM490A steels under various tensile load conditions measured by the single-yoke probe. Although any difference is not observed in the hysteresis loops of 0 (undeformed) and 299 MPa, the hysteresis loops swell and its inclination also toward the horizontal axis beyond the yield strength. The dependence of the magnetomotive force when Φ = 0, NI_c, obtained from the hysteresis loops on tensile stress is shown in Fig. 5. This value NI_c is expected to reflect the variation of coercive force of the steel. The value of NI_c is constant below 450 MPa followed by rapid increase of

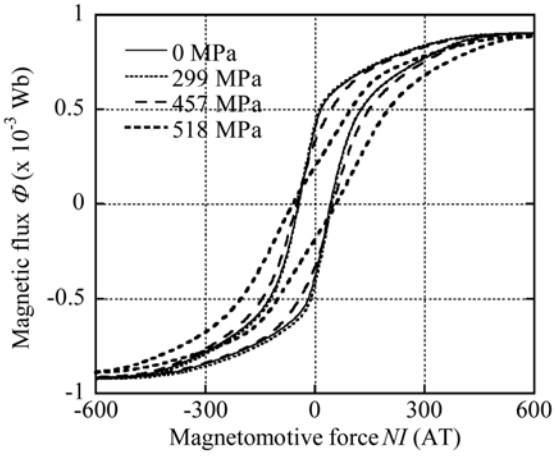

Fig. 4. Hysteresis loops of SM490A steel plates after tensile test.

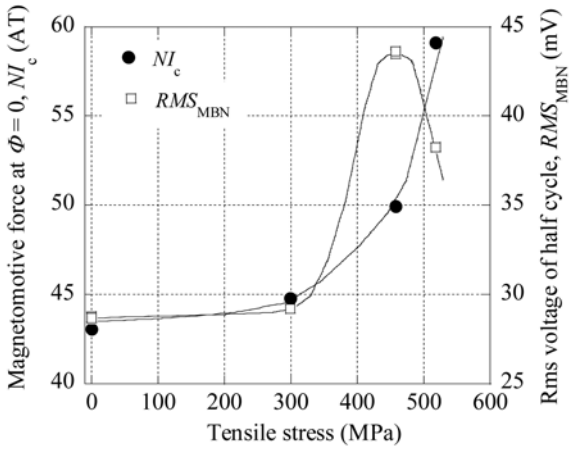

Fig. 5. Dependence of coercive force NI_c, rms voltage RMS_{MBN} on applied tensile stress.

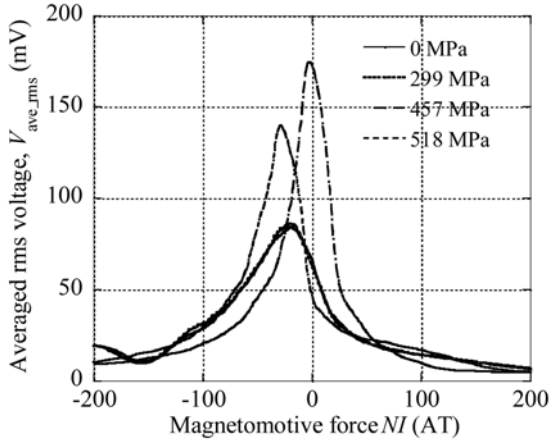

Fig. 6. The profiles of averaged rms voltage V_{rms_ave} against averaged magnetomotive force NI_a.

the parameter above yield strength.

The rms voltage of MBN signals was plotted as a function of the tensile stress in Fig. 5. The rms voltage is also constant up to 450 MPa and then takes a maximum at 457 MPa.

Fig. 6 shows the changes of the averaged rms voltage, V_{rms_ave}, calculated with the moving average method [10] against the averaged magnetomotive force, NI_a for a half cycle of measurement. One can see the appearance of single peak profile in the averaged rms voltage V_{rms_ave} in each plate and the value of magnetomotive force at peak shifts depending on the applied tensile stress.

Fig. 7 shows the peak values in averaged rms voltage, V_p, and the magnetomotive force, NI_p, at which the value of V_{rms_ave} reaches to a peak, for the each tensile stress. The peak value in V_{rms_ave} showed the similar behavior as rms voltage RMS_{MBN} of half cycle measurement, that is, it is constant below yield strength and takes a peak above

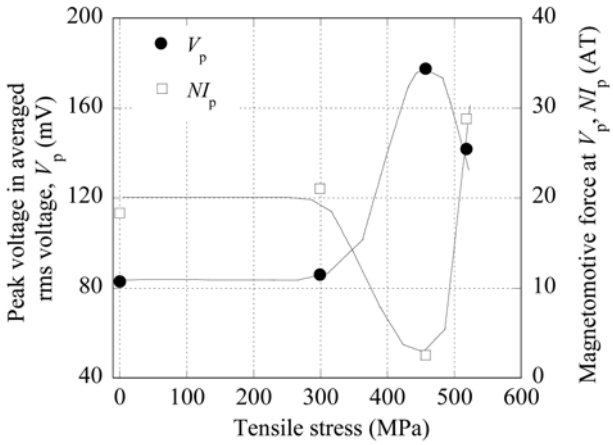

Fig. 7. Dependence of peak in averaged rms voltage V_p and magnetomotive force at peak in averaged rms voltage NI_p on tensile stress.

yield strength. The magnetomotive force at which V_{rms_ave} shows a peak takes a minimum around yield strength and then increases.

4. Discussion

Below 450 MPa, where is in an elastic region, there is no changes in microstructures of the steels after the release of tensile stress. Thus, both coercive force NI_c and rms voltage RMS_{MBN}, are constant in this stage.

Above the yield strength, dislocation density increases monotonically at first, and then dislocations form tangles and cell structures. When cell structures are formed, the number of effective pinning sites for domain wall motion decreases. This is reflected in the variation of the rms voltage RMS_{MBN} of half cycle measurement and the peak value V_p of averaged rms voltage. In Figs. 6 and 7, those parameters increase rapidly above yield strength and then decrease. Therefore, around 518 MPa, microstructures of the steels form cell structure of dislocation. Indeed, we observed the formation of cell structures in the sample applied tensile stress of 518 MPa by Philips-tecnai 30 transmission electron microscope (TEM) as shown in Fig. 8.

The magnetomotive force at peak NI_p of averaged rms voltage means a large number of Barkhausen activity occurs at these magnetic field strength; many domain walls were unpinned at these fields. Therefore these values depend on the intensity of interactions (*i.e.*, pinning force) between pinning sites and domain walls. From the results shown in Fig. 7, the interaction between pinning sites and domain walls becomes weak around yield strength. The dislocation density increases monotonically,

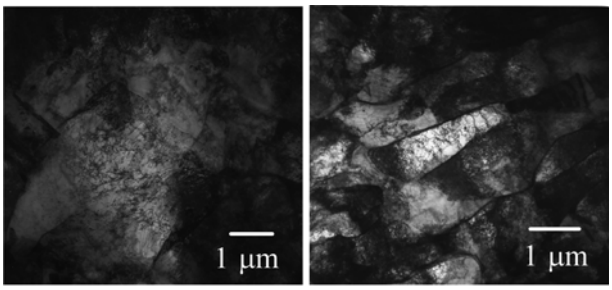

Fig. 8. TEM micrographs showing dislocations and cell structure in SM490A. (a) undeformed specimen: dislocations distribute homogeneously. (b) specimen tensile tested with stress of 518 MPa: dislocations form tangles and cell structures.

however, dislocations distribute non-homogeneously (formation of Lüders band) around yield strength. This causes the distribution of strain field and localized strain field changes. This strain distribution assists to move domain wall easily. As a result, many domain walls may move at weaker field around yield strength.

The coercive force is defined as the magnetic field intensity when the magnetic flux becomes zero. This means the half of total magnetization changes to inverse direction from magnetization saturation state. Since the magnetization process is performed based on domain wall motion and magnetization rotation, the behavior of change of coercive force is affected by both those two magnetization mechanisms. On the other hand, Barkahusen noise reflects only domain wall motions directly, thus, the behaviors of MBN parameters and coercive force is not always consistent.

5. Conclusion

The behaviors of Barkhausen noise parameters and coercive force for the steels applied tensile deformation were investigated. Consequently, the following results are clarified.

(1) Both MBN parameters and coercive force are constant below yield strength due to no changes in microstructures in the elastic region.

(2) The value of rms voltage of half cycle and the peak of averaged rms voltage take a maximum, whereas the magnetomotive force at the peak of averaged rms has a minimum around yield strength. These may reflect the complicated strain distribution when Lüders band is formed in initial plastic region.

(3) The coercive force increases with increasing tensile stress above yield strength. This trend is not consistent with the behavior of MBN parameters. Therefore, it is difficult to explain the change of coercive force based on only interaction of domain wall and pinning sites.

In order to interpret the behaviors of MBN parameters and coercive force in details, further work is to investigate the observation of interaction between domain walls and pinning sites directly by Kerr effect or TEM analysis.

References

[1] D. C. Jiles, Introduction to Magnetism and Magnetic Materials, Chapman & Hall, London (1991).
[2] S. Palit Sagar, N. Parida, S. Das, G. Dobmann, and D. K. Bhattacharya, Int. J. Fatigue **27**, 317 (2005).
[3] D.-G. Park, J.-H. Hong, C.-I. Ok, J.-W. Kim, and H. C. Kim, IEEE Trans. Magn. **34**, 2036 (1998).
[4] C. C. H. Lo, J. Paulsen, and D. C. Jiles, IEEE Trans. Magn. **40**, 2173 (2004).
[5] A. Mitra, Z. J. Chen, F. Laabs, and D. C. Jiles, Philos. Mag. A **75**, 847 (1997).
[6] S. Yamaura, Y. Furuya, and T. Watanabe, Acta Mater. **49**, 3019 (2001).
[7] D. H. L. Ng, K. Cheng, K. S. Cho, Z. Y. Ren, X. Y. Ma, and S. L. I. Chan, IEEE Trans. Magn. **37**, 2734 (2001).
[8] E. R. Kinser, C. C. H. Lo, A. J. Barsic, and D. C. Jiles, IEEE Trans. Magn. **41**, 3292 (2005).
[9] JIS Handbook: Ferrous Materials & Metallurgy II, Japanese Standard Association, Tokyo (2010).
[10] H. Kikuchi, K. Ara, Y. Kamada, and S. Kobayashi, IEEE Trans. Magn. **45**, 2744 (2009).